

Universality and multifractal behaviour of spin-spin correlation functions in disordered Potts models

Christophe Chatelain and Bertrand Berche

Laboratoire de Physique des Matériaux, Université Henri Poincaré Nancy 1,*

B.P. 239, F - 54506 Vandœuvre les Nancy Cedex, France

(August 7, 2018)

We report a transfer matrix study of the random bond q -state Potts model in the vicinity of the Ising model $q = 2$. We draw attention to a precise determination of magnetic scaling dimensions in order to compare with perturbative results. Universality is checked by the computation of the spin-spin correlation function decay exponent obtained with different types of probability distributions of the coupling strengths. Our numerical data, compared to perturbative results for the second moment of the correlation function, obtained with both replica symmetry and replica symmetry breaking schemes, are conclusively in favour of the replica symmetric calculations. The multifractal behaviour of higher moments as well as that of typical correlation functions are also investigated and a comparison is made with the perturbative expansions. Finally, the shape of the correlation function probability distribution is analyzed.

05.20.-y, 05.50.+q, 64.60.Fr

Key Words: Disordered systems, universality, critical exponents, multiscaling

I. INTRODUCTION

Random systems represent the paradigm of spatially inhomogeneous systems where scale invariance is only preserved on average, but not for specific disorder realizations [1]. In such systems, not a single exponent but instead an infinite hierarchy of independent exponents are expected to describe the scaling behaviour of local quantities like order parameter density profiles or correlation functions. This property, linked to the non self-averaging behaviour of the corresponding physical quantities [2–5] is usually referred to as multifractality. The keystone concept which enters the description of multiscaling properties is that of scaling dimensions associated to the moments of the local physical property, or equivalently the universal function $H(\alpha)$ corresponding to the Legendre transform of the set of independent scaling indexes (See e.g. Refs. [6,7]).

Ten years ago already, in a series of illuminating papers, Ludwig [8,9] and Ludwig and Cardy [10] reported an extensive analytic study of 2D random bond Potts ferromagnets in the regime where bond randomness is slightly relevant, q close to 2, q being the number of states per spin. Their studies included perturbative calculations of the conformal anomaly, of the thermal scaling dimension and of the multifractal behaviour of spin-spin correlation functions.

The essential of the numerical studies dealing with scaling dimensions of average quantities in random bond Potts models at small values of q were performed by Monte Carlo (MC) simulations combined to standard Fi-

nite Size Scaling (FSS) [11–14] or transfer matrix (TM) calculations associated to conformal methods [15–19] at the random fixed point (FP) of self-dual disordered models. In particular, an excellent quantitative agreement for the magnetic scaling dimension in the three-state Potts model was reported in Refs. [15,18]. In which concerns the multiscaling properties of spin-spin correlation functions, although some of Ludwig’s predictions have partially been verified both in cylinder geometry [15,20] and in square geometry [21], the agreement with analytical expansions was less conclusive and in particular the shape of the probability distribution has not been reproduced.

Monte Carlo simulations are not convenient to study numerically the vicinity of the Ising model, $q = 2$, where perturbation expansions are supposed to apply. The number of states per spin, q , is indeed restricted to integer values in such simulations. In this paper, we therefore use a rather different approach already used by different authors [15,18,19,22]. This technique is based on the Fortuin-Kasteleyn graph representation [23] which enables TM calculations [24] where q enters as a parameter that can take non integer values. We also benefit from previous studies with a bimodal probability distribution of spin-spin interactions where the disorder amplitude was found to have a deep influence on the measured critical properties in numerical studies [14]. It should thus be chosen carefully in order to avoid crossover perturbations due to the unstable pure model fixed point, $r = 1$, and the percolation fixed point, $r \rightarrow \infty$, r being the ratio between strong and weak couplings.

In this paper, we are mainly interested in the multi-

*Unité Mixte de Recherche CNRS No 7556

scaling behaviour of the spin-spin correlation functions. The first section reminds the reader of the essential relevant theoretical results which have been obtained by several groups using perturbative techniques around the pure models conformal field theories. Section III explains the methodology and section IV gives the numerical results:

- i) Universality in quenched disordered ferromagnetic Potts models is checked using different types of probability distributions of nearest-neighbour couplings.
- ii) The numerical study of the decay exponent of the second moment of the spin-spin correlation function is then compared to perturbative results in order to test Replica Symmetry and Replica Symmetry Breaking scenarios.
- iii) Finally, we study other moments and deduce the shape of the universal functions $H(\alpha)$ for different q values. The probability distribution of spin-spin correlation functions is also analyzed.

The values of q are chosen in the range 2 to 4, where the pure model exhibits a second order phase transition, with a special attention paid on the neighbourhood of $q = 3$.

II. SUMMARY OF THE PERTURBATION RESULTS

A. The 2D random Ising model

According to the celebrated Harris criterion [25], quenched randomness is a marginal perturbation in the 2D Ising model. This situation has focused a considerable interest on the critical properties of the random bond Ising model (RBIM), and, after partially conflicting results, disorder was eventually found to be marginally irrelevant, leading to an unchanged universal behaviour apart from logarithmic corrections for the ensemble average of some physical quantities [26–31]. These results were then carefully checked through intensive MC simulations [32–34] and series expansions [35–37]. We mention that site dilution is still subject to controversial interpretations (See e.g. Ref. [37]) in spite of a conclusive recent work leading to the same conclusions than bond randomness [38].

The free energy density in a strip of width L with periodic boundary conditions was obtained by Ludwig and Cardy [10]:

$$\overline{f(L)} \simeq f_0 - \frac{\pi}{6L^2} \left(\frac{1}{2} - 128\pi^3 \Delta^3 (1 + 8\pi\Delta \ln L)^{-3} \right), \quad (1)$$

where Δ , the variance of the Gaussian probability distribution of exchange interactions, is the strength of disorder related to the ratio r . In this expression, overbar

denotes the disorder average. The central charge c , defined by the leading size dependence of the free energy density in the cylinder geometry, $\frac{\pi c}{6L^2}$, thus exhibits logarithmic corrections which make its exact value $\frac{1}{2}$ difficult to extract numerically [39].

Using a perturbation expansion, Ludwig later obtained the behaviour of the moments of the spin-spin correlation function [9]:

$$\overline{\langle \sigma(0)\sigma(\rho) \rangle^p} \simeq \rho^{-p/4} (\Delta \ln \rho)^{p(p-1)/8} \quad (2)$$

when Δ , the strength of disorder, is strong enough. Brackets denote the thermal average. We can also introduce a reduced correlation function whose leading power-law behaviour is

$$\overline{\langle \sigma(0)\sigma(\rho) \rangle^p}^{1/p} \sim \rho^{-2x_\sigma}. \quad (3)$$

Ludwig's results imply that logarithmic corrections are absent in the case of the average correlation function ($p = 1$), $\overline{\langle \sigma(0)\sigma(\rho) \rangle} \sim \rho^{-1/4}$, while typical correlation functions ($p = 0$) exhibit such corrections, $\exp \overline{\ln \langle \sigma(0)\sigma(\rho) \rangle} \sim \rho^{-1/4} (\Delta \ln \rho)^{-1/8}$, observed numerically [40]. Furthermore, a unique scaling dimension $x_\sigma = \frac{1}{8}$ describes the leading power-law decay of all the moments of the spin-spin correlation function, $\overline{\langle \sigma(0)\sigma(\rho) \rangle^p} \sim \rho^{-2px_\sigma}$, and no multiscaling behaviour is expected apart from the logarithmic correction term.

The surface correlation function has also been studied recently and was found to be self-averaging [41].

B. The random bond Potts model

In the case of the Potts model with $q > 2$, disorder is a relevant perturbation which modifies the universal critical behaviour and leads to new fixed point critical properties. Studying the effect of a slightly relevant perturbation on the finite-size scaling behaviour of the free energy density in a strip geometry of width L at the new fixed point, Ludwig and Cardy [10], obtained perturbatively the central charge $c'(q)$ of the 2D q -state Potts model with weak quenched bond randomness (here and in the following, primes denote the central charge and the critical exponents at the disordered fixed point, while unprimed symbols refer to the pure fixed point quantities). Using an expansion in $q - 2$ around the Ising model, the random anomaly was deduced from the random free energy of the strip,

$$f(L, g^*) = A - \frac{\pi c'(q)}{6L^2} + O(L^{-3}), \quad (4)$$

given in the replica formalism by the quenched free energy $\partial f(n)/\partial n|_{n \rightarrow 0}$:

$$c'(q) = \frac{1}{2} \left(1 + \frac{7}{4} y_H - \frac{9}{16} y_H^2 - \frac{5}{64} y_H^3 + O(y_H^4) \right), \quad (5)$$

where y_H is the renormalization group (RG) eigenvalue associated to the bond disorder [25], $y_H = \alpha/\nu = 2 - 2x_\varepsilon(q)$, $x_\varepsilon(q)$ being the scaling dimension of the energy density in the pure model¹. This latter dimension is obtained for arbitrary $q \leq 4$ by the den Nijs conjecture [42,43], rigourously proved by Dotsenko and Fateev [44]:

$$x_\varepsilon(q) = \frac{1+\mu}{2-\mu}, \quad 0 \leq \mu = \frac{2}{\pi} \cos^{-1}(\tfrac{1}{2}\sqrt{q}) \leq 1, \quad (6)$$

and to lowest order, the RG eigenvalue is proportional to $q-2$: $y_H = \frac{4}{3\pi}(q-2) + O[(q-2)^2]$. The deviation of the conformal anomaly from its pure fixed point value,

$$c(q) = 1 - \frac{3\mu^2}{2-\mu}, \quad (7)$$

is difficult to measure, since it is only of third order in y_H and it requires a very good accuracy to distinguish between pure and random values.

The thermal exponent was similarly obtained to two-loop order by Ludwig [8]:

$$\begin{aligned} x'_\varepsilon(q) &= x_\varepsilon(q) + \frac{1}{2}y_H + \frac{1}{8}y_H^2 + O(y_H^3) \\ &= 1 + \frac{1}{8}y_H^2 + O(y_H^3), \end{aligned} \quad (8)$$

and the three-loop correction was reported by Jug and Shalaev [45].

The correction to the magnetic exponent requires a three-loop calculation. It was obtained by Dotsenko et al [46]

$$x'_\sigma(q) = x_\sigma(q) + \frac{1}{32} \frac{\Gamma^2(-\frac{2}{3})\Gamma^2(\frac{1}{6})}{\Gamma^2(-\frac{1}{3})\Gamma^2(-\frac{1}{6})} y_H^3 + O(y_H^4), \quad (9)$$

and checked by Picco using MC simulations [12]. In contradistinction with the thermal exponent, the deviation

from the pure fixed point value is quite small close to $q=2$.

Searching for multiscaling properties, Ludwig obtained, up to linear order, the scaling dimension of the p^{th} -moment² [9] of the reduced spin-spin correlation function, $\overline{\langle \sigma(0)\sigma(\rho) \rangle^p}^{1/p} \sim \rho^{-2x'_{\sigma p}(q)}$ and Lewis performed recently the computation up to the second order [47,48]

$$\begin{aligned} x'_{\sigma p}(q) &= x_\sigma(q) - \frac{1}{16}(p-1)y_H \\ &\quad - \frac{1}{32}(p-1)[A + B(p-2)]y_H^2 + O(y_H^3), \end{aligned} \quad (10)$$

where $A = \frac{11}{12} - 4 \ln 2$ and $B = \frac{1}{24}(33 - 29\sqrt{3}\pi/3)$. Here, the exponent corresponding to the *average* critical correlation function at the random fixed point is denoted by $x'_{\sigma 1}(q) \equiv x'_\sigma(q)$, while the *typical* behaviour corresponds to $p=0$. This result, obtained in the Replica Symmetry (RS) scenario, contains the special case of the second moment performed by Dotsenko et al [49] in order to compare between Replica Symmetry

$$\begin{aligned} x'_{\sigma^2}(q) &= x_\sigma(q) - \frac{1}{16}y_H \\ &\quad + \frac{1}{32} \left(4 \ln 2 - \frac{11}{12} \right) y_H^2 + O(y_H^3), \end{aligned} \quad (11)$$

and Replica Symmetry Breaking (RSB)³ [50]:

$$\begin{aligned} x''_{\sigma^2}(q) &= x_\sigma(q) - \frac{1}{16}y_H \\ &\quad + \frac{1}{32} \left(4 \ln 2 - \frac{5}{12} \right) y_H^2 + O(y_H^3), \end{aligned} \quad (12)$$

¹In this paper, we use the notations of Refs. [8–10]: The expansion parameter is y_H . It is related to the parameter ϵ , linked to the deviation from the pure Ising model central charge, used by Dotsenko and co-workers in Refs. [46,47,49,50] by $y_H = 3\epsilon$.

²In the literature, many different notations have been used for the scaling dimensions of the moments of the correlation functions. Our notation corresponds to that of Lewis [48]: $x'_{\sigma p} \leftrightarrow \Delta'_{\sigma p}$. The correspondence with other works is the following: Ludwig [9]: $x'_{\sigma p} \leftrightarrow X_N/N$, Dotsenko et al [49]: $x'_{\sigma^2} \leftrightarrow \Delta'_{\sigma^2}/2$ and Olson and Young [21]: $x'_{\sigma p} \leftrightarrow \eta_n/2$.

³In Ref. [50], the thermal and magnetic exponents have been computed with both RS and RSB scenarios. While Eq. (9) for the average behaviour is unchanged up to the third order in the RSB scheme, the thermal exponent in Eq. (8) becomes $x'_\varepsilon(q) = 1 + O(y_H^3)$.

III. MODEL AND METHODOLOGY

In this paper, we consider Potts-spin variables, $\sigma_j \in 1, 2, \dots, q$ on the sites of a square lattice with independent quenched random nearest-neighbour ferromagnetic interactions K_{ij} . These exchange couplings are taken from a probability distribution $\mathcal{P}(K_{ij})$, and in most of our applications, they can take two values, $K_1 = K$, $K_2 = rK$, $r > 1$ with equal probabilities:

$$\mathcal{P}(K_{ij}) = \frac{1}{2}\delta(K_{ij} - K) + \frac{1}{2}\delta(K_{ij} - rK), \quad (13)$$

where r measures the strength of disorder. Our methodology will be discussed in this section with the particular case of probability distribution (13) and the generalization to other distributions will be presented in the next section.

The Hamiltonian of the model is thus written

$$-\beta\mathcal{H} = \sum_{(i,j)} K_{ij} \delta_{\sigma_i, \sigma_j}. \quad (14)$$

We only consider self-dual models for which the critical point is exactly known. In the case of the bimodal distribution (13), the self-duality point

$$[\exp(K_c(r)) - 1][\exp(rK_c(r)) - 1] = q, \quad (15)$$

corresponds to the critical point of the model if only one phase transition takes place in the system as rigourously shown in Ref. [51].

The degree of dilution in the system can be varied by changing the ratio of the strong and weak couplings, r . At $r = 1$, one recovers the perfect q -state Potts model, whereas for $r \rightarrow \infty$ we are in the percolation limit, where $T_c = 0$. The intermediate regime of dilution $1 < r < \infty$ is expected to be controlled by the random fixed point located at some $r = r^*(q)$ [19]. This optimal disorder amplitude, $r^*(q)$, can be obtained numerically from the maximum condition of the effective central charge of the disordered system. Dotsenko and co-workers for example considered n q -state Potts models coupled via energy-energy interactions and obtained perturbatively the central charge deviation from the decoupling limit (where c is given by the sum of the central charges of the decoupled models) [52]: $\Delta c = -\frac{1}{8} \frac{n(n-1)}{(n-2)^2} y_H^3 + O(y_H^4)$. For $n > 1$, Δc satisfies the Zamolodchikov's c -theorem according to which there exists a c -function decreasing along RG flows and giving the central charge at the fixed point [53]. In the case of random systems ($n \rightarrow 0$ in the replica approach), the central charge increases and can be expected to reach a maximum value at an optimal disorder amplitude where the random FP exponents may be extracted from numerical data. This property, linked to non-unitarity in the presence of disorder, is indeed observed in simulations [15,19,22].

In the following we used a TM technique, based on the Blöte and Nightingale connectivity transfer matrix [24],

which enables to compute the physical quantities in long cylinders. Since transfer operators in the time direction do not commute in disordered systems, the free energy density is defined by the leading Lyapunov exponent. For an infinitely long strip of width L with periodic boundary conditions, the leading Lyapunov exponent is given by the Furstenberg method [54]:

$$\Lambda_0(L) = \lim_{m \rightarrow \infty} \frac{1}{m} \ln \left\| \left(\prod_{k=1}^m \mathbf{T}_k \right) |v_0\rangle \right\|, \quad (16)$$

where \mathbf{T}_k is the transfer matrix and $|v_0\rangle$ is a unit initial vector. The quenched free energy density is thus given by

$$\overline{f(L)} = -L^{-1} \Lambda_0(L). \quad (17)$$

The shape of the central charge as a function of the disorder amplitude is shown in Fig. 1 for several values of q . Each realization of disorder is obtained via 10^6 iterations of the transfer matrix and the free energy density was averaged over 96 such realizations.

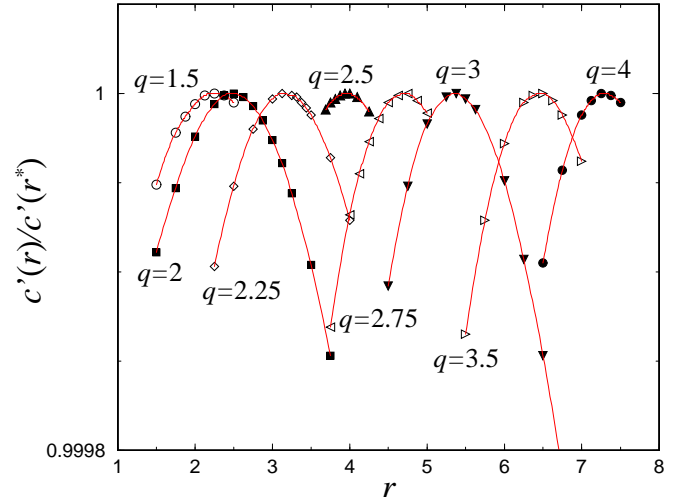


FIG. 1. Behaviour of the central charge as a function of the disorder amplitude for different values of the number of states q (binary distribution of Eq. (13)). The solid lines are parabolic fits. The maximum corresponds to the optimal value of disorder amplitude.

TABLE I. Optimal disorder amplitude and corresponding values of the central charges of the disordered Potts model for different values of q for the binary probability distribution in Eq. (13). The last columns give the numerical values of the pure model central charge $c(q)$ (Eq. (7)) and of the expansion parameter used in the perturbation results, and shows that the perturbation expansion obviously breaks down when q increases.

q	$r^*(q)$	$c'(q)$		$c(q)$	y_H
		TM result	Eq. (5)		
1.5	2.25	0.283(1)		0.288	
2.	2.49	0.496(6)	0.5	0.500	0.
2.25	3.18	0.584(8)	0.5876	0.588	0.1036
2.5	3.96	0.662(8)	0.6661	0.666	0.2036
2.75	4.70	0.732(8)	0.7371	0.736	0.3017
3.	5.36	0.797(8)	0.8020	0.800	0.4000
3.25	5.94	0.857(9)	0.8617	0.858	0.5013
3.5	6.45	0.912(11)	0.9174	0.910	0.6101
4.	7.30	1.011(12)	1.0312	1.000	1.

The central charge follows from a polynomial fit

$$\overline{f(L)} = f_0 - \frac{\pi c}{6L^2} + A_4 L^{-4} + A_6 L^{-6} + A_8 L^{-8}, \quad (18)$$

where the remaining coefficients A_i have been included in order to simulate finite size effects, although the exact dependence of corrections to scaling is not known. The calculations were performed on strips of widths $L = 2$ to 8. The central charge is still sensible to the number of disorder configurations entering the average and to the degree of the polynomial fit. Nevertheless, it is expected that the position of the maximum presents small enough deviations for the critical exponents to reflect the disordered fixed point regime in the neighbourhood of this maximum. We have checked different types of fits, with less parameters and also including logarithmic terms in the vicinity of $q = 2$ where equation (1) is supposed to be valid, but we were not able to improve the results, since, as it has already been observed [15], the values of $c'(q)$ are systematically below the perturbative result of Ludwig and Cardy [10], and even below the pure model central charge at small values of q . In all the cases, the error can be estimated by the fluctuations of the results with different fitting procedures and it is of order 10^{-3} to 10^{-2} . For example we obtain $c'(2) = 0.496$ with Eq. (18), 0.492 with $A_6 = A_8 = 0$, 0.497 with $A_8 = 0$ but a $(\ln L)^{-3}$ term added or 0.495 with $A_6 = A_8 = 0$ and the log-term present. The error bars given in table I correspond to the fluctuations of the results obtained with the different fits. The maximal values and optimal disorder amplitude $r^*(q)$ are also given in table I.

For a specific disorder realization, the spin-spin correlation function along the long direction, u , of the strip

$$\langle \sigma(j) \sigma(j+u) \rangle = \frac{q \langle \delta \sigma_j \sigma_{j+u} \rangle - 1}{q - 1}, \quad (19)$$

where $\langle \dots \rangle$ denotes the thermal average, is given by a product of non-commuting transfer matrices. They were computed on strips of widths $L = 2$ to 8 and then averaged over 80 000 disorder realizations.

We will now assume that conformal covariance can be applied to the order parameter correlation function and its moments. In the infinite complex plane $z = x + iy$ the correlation function and its moments exhibit the usual algebraic decay at the critical point

$$\overline{\langle \sigma(z_1) \sigma(z_2) \rangle}^p = \text{const} \times \rho^{-2x'_{\sigma p}(q)}, \quad (20)$$

where $\rho = |z_1 - z_2|$. Multiscaling arises when the exponents $x'_{\sigma p}(q)$ are all different, depending upon the value of the moment order p , and their p -dependence is a convex function [9]. Under the logarithmic transformation $w = \frac{L}{2\pi} \ln z = u + iv$ which maps the infinite plane geometry inside an infinitely long strip of width L , one gets the exponential decay along the strip

$$\overline{\langle \sigma(j) \sigma(j+u) \rangle}^p = \text{const} \times \exp \left[-\frac{2\pi}{L} x'_{\sigma p}(q) u \right]. \quad (21)$$

The scaling dimensions $x'_{\sigma p}(q)$ at different strip sizes can thus be deduced from an exponential fit, and a quadratic extrapolation at $L \rightarrow \infty$ is performed to get the corresponding value in the thermodynamic limit. The calculation of errors follows the lines explained in Ref. [19].

This method was used in Ref. [19] for the average correlation function, i.e. for $p = 1$, and in the large q regime. In this work, we calculate the higher moments, as well as the typical behaviour, governed by the derivative of the exponent $x'_{\sigma p}$ with respect to p , evaluated in the limit $p \rightarrow 0$. In previous works, it was shown that the results from exponent extrapolations are sensitive to the value of the disorder strength chosen for the simulation, since the finite size corrections are very strong unless the calculations are performed close to the random fixed point [14] as obtained from the maximum condition of the central charge of the model [19,52]. Our simulations were performed at these fixed point values of the disorder strength, but for comparison we have also considered systems with somewhat different values.

Since the correlation functions are not self-averaging, the disorder average must be performed carefully. We follow the same procedure as in Ref. [19] where we compared the ensemble average $\overline{\langle \sigma(0) \sigma(u) \rangle}$ to a cumulant expansion in terms of the moments of $\ln \langle \sigma(0) \sigma(u) \rangle$, which are self-averaging [15]:

$$\overline{\langle \sigma(0) \sigma(u) \rangle}^p = \exp \left[p \overline{\ln \langle \sigma(0) \sigma(u) \rangle} + \frac{1}{2} p^2 \left(\overline{(\ln \langle \sigma(0) \sigma(u) \rangle)^2} - \overline{\ln \langle \sigma(0) \sigma(u) \rangle}^2 \right) + \dots \right]. \quad (22)$$

Although the average should in principle be done using the cumulant expansion, we observe that the direct average, which is compatible with the cumulant expansion,

is more stable than this latter expansion. This is particularly true at high moment orders and is probably due to the large number of disorder realizations used in the calculations. This is illustrated for several moments at $q = 3$ in Fig. 2 where the solid lines represent the direct average over 96 000 different samples, while the open symbols correspond to the cumulant expansion up to the fifth order.

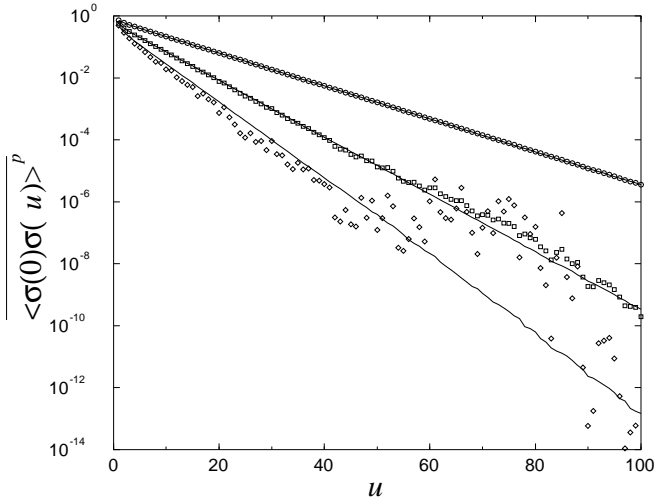


FIG. 2. Moments of the spin-spin correlation function $p = 1, 2$ and 3 from upper to lower curves ($q = 3$, $L = 7$, $r = 5.36$). The solid lines correspond to the average over 96 000 different disorder realizations and the symbols are deduced from the cumulant expansion up to the fifth order. The fluctuations become extremely large above the fifth order. Both solid lines and symbols give the same order for the corresponding scaling dimensions (related to the slopes of these curves), but the direct average leads to more precise results.

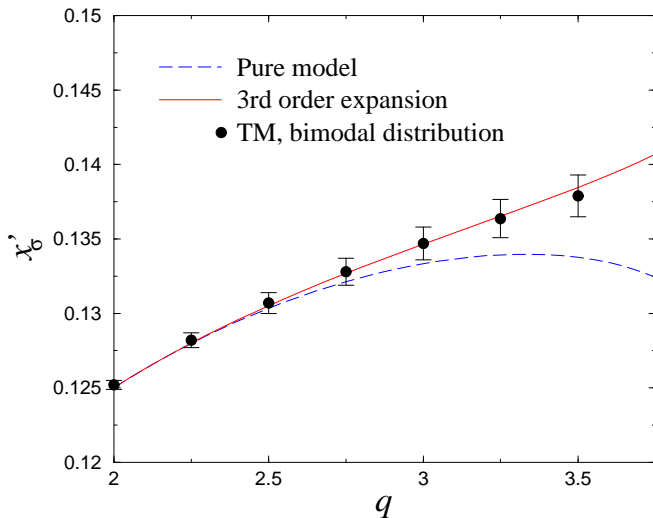


FIG. 3. Scaling dimension of the order parameter (binary disorder) compared to the third order expansion of Dotsenko and co-workers [46]. The scaling dimension corresponding to the pure model is shown for comparison.

From the exponential decay of the average correlation function, the exponent $x'_\sigma(q)$ is deduced and presented as a function of q for the case of a binary disorder in Fig. 3. Although these results are not new, since the same type of curve was reported by Cardy and Jacobsen in Ref. [18], the agreement with our results confirms the reliability of the averaging procedure. The results are compared to the third order expansion of Dotsenko *et al* [46] in Eq. (9). The data themselves are given in table II. The agreement is extremely good especially in the region where the expansion is supposed to be valid when q is not too far from the Ising model value $q = 2$.

TABLE II. Comparison of the numerical results for the magnetic scaling dimension (bimodal probability distribution) $x'_\sigma(q)$ with the third order expansion of Dotsenko and co-workers [46]. The error bars systematically contain the analytical value.

q	x'_σ	
	Expansion (9)	TM result
2	0.12500	0.1252(3)
2.25	0.12800	0.1282(5)
2.5	0.13051	0.1307(7)
2.75	0.13269	0.1328(9)
3.	0.13465	0.1347(11)
3.25	0.13653	0.1364(13)
3.5	0.13845	0.1379(14)

Even close to the marginally irrelevant case of the Ising model where logarithmic corrections are known to be present for some quantities, we note that the numerical data are quite satisfactorily in agreement with the perturbative results. This is due to the absence of logarithmic corrections for the *average* correlation function at $q = 2$, and we will see that this observation is no longer true in the following study of other moments.

IV. TESTS OF UNIVERSALITY

A. Universality of the average behaviour

The question of universality in random systems is not yet solved, especially when frustration occurs, like in random fields or spin glasses [55]. We address in this section the question of the influence of the particular shape of the probability distribution of exchange couplings on the universality class. There are still subsisting doubts concerning universality since incompatible estimations (taking error bars into account) of the critical exponent x'_σ were obtained with different probability distributions. For ex-

ample at $q = 8$, the choice of a bimodal probability distribution led to 0.151(4) [14] (FSS) or 0.1505(3) [19] (conformal invariance), while a continuous distribution gave 0.161(3) [21] (FSS).

In this section, we show that the discrepancy is simply due to crossover effects but does not imply absence of universality. Following the methodology of the previous sections, the disordered fixed point regime is located at the maximum of the central charge and the scaling dimension x'_σ of the average spin-spin correlation functions is estimated. The results of Fig. 3 are considered as a reference and the same method is applied to ternary, quaternary and continuous distributions and is shown to lead to identical critical exponents, within error bars, to those of a binary distribution.

1. Ternary distribution

The ternary probability distribution is defined by

$$\mathcal{P}(K_{ij}) = \frac{1}{3} [\delta(K_{ij} - K_0) + \delta(K_{ij} - K) + \delta(K_{ij} - rK)] \quad (23)$$

with the self-duality condition

$$[\exp(K_c(r)) - 1][\exp(rK_c(r)) - 1] = [\exp(K_0) - 1]^2 = q, \quad (24)$$

where $K_0 = \ln(1 + \sqrt{q})$ is the critical coupling of the pure system. The homogeneous system corresponds to the value $r = 1$. We tried different kinds of interpolation procedures for the free energy, as in Eq. (18), but always found a monotonic variation of the corresponding central charge with respect to the disorder amplitude r . The absence of maximum might be the sign of the presence of strong corrections, possibly due to the fact that one third of the exchange couplings keeps their pure value K_0 even in the infinite-disorder limit. Nevertheless, we present in the table III the magnetic exponent as extracted from the average spin-spin correlation functions for different values of r .

TABLE III. Scaling dimension x'_σ of the average order parameter for the $q = 3$ Potts model with a ternary distribution compared to the results for a binary distribution at the optimal disorder amplitude and for the pure model.

Distribution	disorder amplitude	$x'_\sigma(3)$
Pure	$r = 1$	0.1333
Binary	$r^* \simeq 5.363$	0.1347(11)
Ternary	$r = 2$	0.1339(3)
	$r = 4$	0.1343(6)
	$r = 5.363$	0.1344(8)
	$r = 8$	0.1344(10)
	$r = 12$	0.1343(13)
	$r = 20$	0.1341(15)

For strong disorder, the scaling dimension x'_σ , as presented in the table III, shows a plateau with a value compatible within error bars with that of the binary distribution, but the agreement is not yet conclusive, since the effective central charge was not found to display a clear maximum.

2. Quaternary distribution

The quaternary probability distribution is defined by

$$\mathcal{P}(K_{ij}) = \frac{1}{4} [\delta(K_{ij} - K) + \delta(K_{ij} - rK) + \delta(K_{ij} - K') + \delta(K_{ij} - r^2 K')] \quad (25)$$

where the four equi-probable exchange couplings K , rK , K' and $r^2 K'$ are related by

$$\begin{aligned} & [\exp(K_c(r)) - 1][\exp(rK_c(r)) - 1] \\ &= [\exp(K'_c(r)) - 1][\exp(r^2 K'_c(r)) - 1] = q \end{aligned} \quad (26)$$

at the self-dual point of the model. The value $r = 1$ corresponds to the pure system and the limit $r \rightarrow +\infty$ to a percolative regime.

As seen on figure Fig. 4, the central charge presents both a maximum at $r^* \simeq 2.000$ and a “minimum” at $r_* \simeq 3.763$. According to Zamolodchikov’s c -theorem in the case of non-unitary theories, the latter case should correspond to an instable fixed point while the former situation is likely to be the disordered fixed point.

In table IV, we collect the scaling dimensions of the average spin-spin correlation functions at these two fixed points and, for comparison, those of the pure model and of the disordered system with a binary distribution.

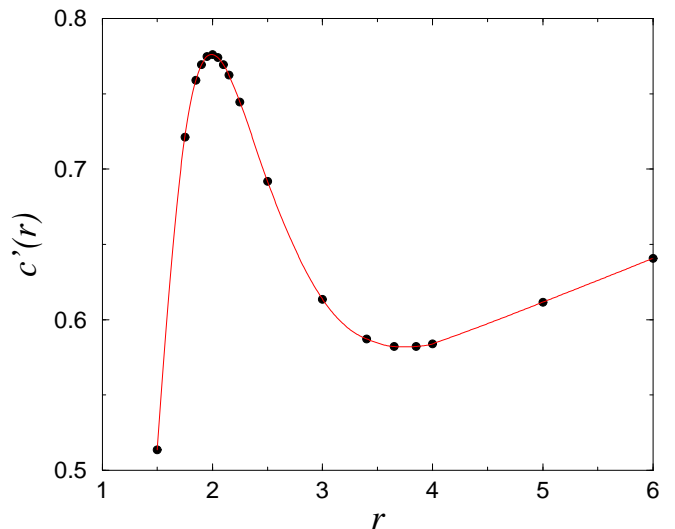


FIG. 4. Behaviour of the central charge as a function of the disorder amplitude r for the quaternary distribution (25) at $q = 3$. The dotted curve is a guide for the eyes.

TABLE IV. Scaling dimensions x'_σ ($q = 3$) of the average order parameter for the two extrema (r^* (written in bold face) and r_*) of the central charge with a quaternary distribution compared to the results for the binary case and for the pure model.

Distribution	disorder amplitude	$x'_\sigma(3)$
Pure	$r = 1$	0.1333
Binary	$r^* \simeq \mathbf{5.363}$	0.1347(11)
Quaternary	$r^* \simeq \mathbf{2.000}$	0.1343(6)
	$r_* = 3.763$	0.0097(12)

Inspection of the results in table IV reveals that compatible exponents are obtained at the maximum of the central charge with both probability distributions. These data also confirm once again that the disorder amplitude r plays an essential role [14], since the value at r_* is definitely excluded by the perturbative result.

3. Continuous distribution

Recently, Olson and Young [21] proposed slightly different numerical estimations of the critical exponents of the average magnetization and of its first moments, compared to other independent studies [20,19,48]). They used an interesting continuous probability distribution of exchange couplings that they claimed to be less sensible to crossover effects. We show in the following that the randomness amplitude chosen in the simulations of Olson and Young is not the optimal one, since it is not strong enough to reach the disordered fixed point. This observation may be at the origin of the slight discrepancy between the extrapolated values of the exponents.

The continuous probability distribution used by Olson and Young is generalized by introduction of a parameter $r = e^\lambda$ which controls the strength of randomness. Following their notation, we have chosen the distribution

$$\mathcal{P}(y_{ij}) = \frac{1}{\cosh \frac{y_{ij}}{\lambda}} \quad (27)$$

where

$$e^{y_{ij}} = \frac{e^{K_{ij}} - 1}{\sqrt{q}}. \quad (28)$$

Self-duality is ensured by the parity of the distribution $\mathcal{P}(y_{ij})$. The definition of the disorder amplitude r is such that $r = 1$ corresponds again to the pure system and $r = e$ to the Olson-Young distribution. The probability distribution of exchange couplings K_{ij} is given by

$$\mathcal{P}(K_{ij}) = 2 \frac{q^{1/2\lambda}}{\pi\lambda} \frac{e^{K_{ij}}(e^{K_{ij}} - 1)^{1/\lambda-1}}{q^{1/\lambda} + (e^{K_{ij}} - 1)^{2/\lambda}} \quad (29)$$

and can be generated by the formula

$$K_{ij} = \ln \left(1 + \sqrt{q} \tan^\lambda \frac{\pi x}{2} \right) \quad (30)$$

if $x \in [0; 1[$ is a uniformly distributed random variable. Examples of probability distributions at different disorder amplitudes are shown in Fig. 5.

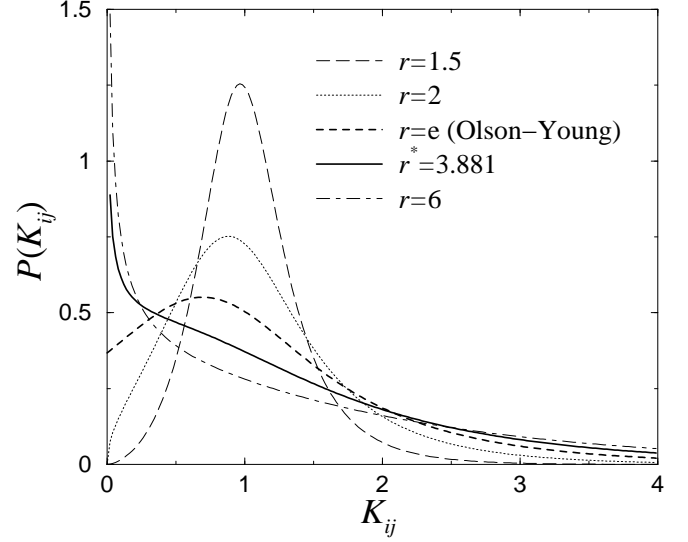


FIG. 5. Probability distribution of exchange couplings $\mathcal{P}(K_{ij})$ for disorder amplitudes r in the range $[1.5; 6]$.

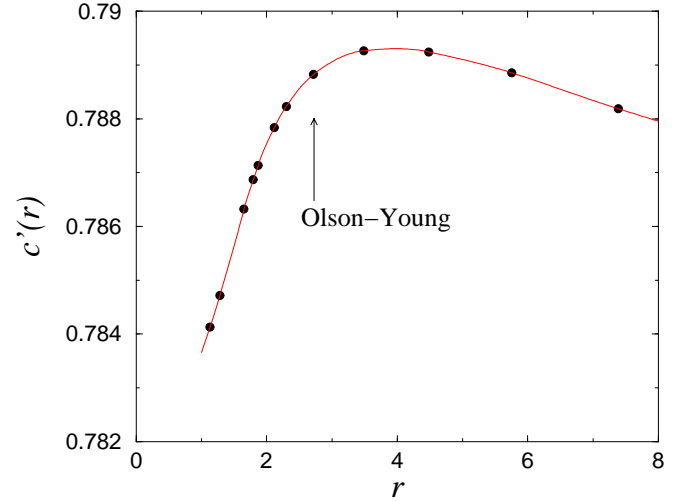


FIG. 6. Central charge of the $q = 3$ random bond Potts model for the continuous distribution Eq. (29) with respect to the disorder amplitude r .

The maximum of the central charge is found in Fig. 6 at the amplitude of disorder $r^* \simeq 3.881$. The scaling dimension of the average order parameter, obtained at r^* , is given in table V and compared to other disorder amplitudes. Again, there is a convincing agreement with the results obtained with the binary distribution.

With the continuous distribution at $r = e$, Olson and Young measured slightly higher values for different values of q . We propose here a possible explanation of the small discrepancy: It was shown that the larger the number of state q of the Potts model the stronger the disorder should be to reach the disordered fixed point regime [14,19,56]. Thus, for $q \geq 3$ random bond Potts models, the *ideal* disorder amplitude should become larger and larger, far from the value $r = e \simeq 2.718$ implicitly used by Olson and Young. On the other hand, since in the weak disorder regime the average exponent is continuously growing with the disorder amplitude r , a too weak randomness cannot be the explanation of the slightly too high values for the exponents obtained by Olson and Young. A possible origin of the small disagreement can be found in the ensemble average: If the number of disorder realizations is too small, the average behaviour will give an exponent closer to the typical one, and thus too large.

TABLE V. Scaling dimension x'_σ of the average order parameter for the $q = 3$ random bond Potts model with a continuous distribution at the optimal disorder amplitude (written in bold face) and other amplitudes as well, compared to the results obtained in the binary case and for the pure model.

Distribution	disorder amplitude	$x'_\sigma(3)$
Pure	$r = 1$	0.1333
Binary	$r^* \simeq \mathbf{5.363}$	0.1347(11)
Continuous	$r = 1.133$	0.1338(1)
	$r = e$	0.1340(9)
	$r^* \simeq \mathbf{3.881}$	0.1344(13)
	$r = 7.389$	0.1348(17)

B. Replica Symmetry

The question of a possible breaking of replica symmetry [57] in disordered systems is very controversial and far from being settled, especially in spin glasses (see e.g Refs. [58–61]). In the context of disordered Potts ferromagnets, the question was first asked by Dotsenko et al [49]. The Hamiltonian (14) is rewritten

$$\begin{aligned}
-\beta\mathcal{H}[\sigma] &= K_0 \sum_{(i,j)} \delta_{\sigma_i, \sigma_j} + \sum_{(i,j)} (K_{ij} - K_0) \delta_{\sigma_i, \sigma_j} \\
&= -\beta\mathcal{H}_0[\sigma] - \beta\mathcal{H}'[\sigma]
\end{aligned} \tag{31}$$

where the deviation from the pure system can be written in the continuum limit

$$-\beta\mathcal{H}' \sim \int \tau(x) \epsilon(x) d^2x \tag{32}$$

with $\tau(x) = K(x) - K_c$. The average free energy $\overline{F} = -k_B T \ln \overline{Z}$ can be obtained using the identity

$\overline{\ln Z} = \lim_{n \rightarrow 0} \frac{\overline{Z^n} - 1}{n}$ by introduction of n identical copies (labelled by an index a) of the model, coupled by their energy densities. After integration over a Gaussian probability distribution centered on the value τ_0 and with variance Δ , one is led to:

$$\begin{aligned}
\overline{Z^n} &= \text{Tr} \exp \left[-\beta \sum_a \mathcal{H}_0^{(a)} + \tau_0 \int d^2x \sum_a \epsilon_a(x) \right. \\
&\quad \left. + \Delta \int d^2x \sum_{a \neq b} \epsilon_a(x) \epsilon_b(x) \right]
\end{aligned} \tag{33}$$

The first term governed by the average coupling τ_0 produces a shift in the critical temperature, while the second term couples the replicas with each other. In a replica symmetric scenario, the couplings Δ between the different copies of the model are identical, while in a Replica Symmetry Breaking scheme, these couplings are Parisi matrices and can take different values Δ_{ab} . Treated as a perturbation this coupling term leads to different fixed point structures and finally to different scaling dimensions for the moments of the correlation functions. In order to test between Replica Symmetry and Replica Symmetry Breaking schemes, Dotsenko et al performed a second order expansion of the exponent of the second moment of the spin-spin correlation function decay in both cases (Equations (11) and (12)). Previous MC simulations have been performed at $q = 3$ but were not completely conclusive, although in favour of Replica Symmetry: The perturbation expansion leads to $x'_{\sigma^2}(3) = 0.1176$ and $x''_{\sigma^2}(3) = 0.1201$ according to Eq. (11) and (12), while previous numerical results lead to 0.113(1) [49], 0.1140(5) [48], 0.116(1) [20] and 0.119(2) [21].

In this section, we report new conclusive results for different values of q . Close to $q = 2$, the proximity of the marginally irrelevant Ising FP will surely alter the data, as a reminiscent effect of the logarithmic corrections present exactly at $q = 2$ for the second moment. Too large values of q on the other hand are not very helpful in order to check perturbation expansions which break down when one explores higher values of the expansion parameter (as given for example in table I). One thus has to balance these two extreme situations and the comparison between numerical data and perturbation results should be conclusive around $q = 3$. The TM technique thus appears to be well adapted, since it is capable to deal with non integer values of q .

The comparison is shown in Fig. 7 for the bimodal probability distribution and the results are also given in table VI. In the convenient domain for the test, around $q = 3$, results are written in bold face. The agreement with Replica Symmetry is quite convincing for the bimodal probability distribution. We note that with the continuous distribution of Eq.(29), we obtain also a very good value at $q = 3$: 0.1173(14) and with the ternary distribution at $r = 8$ we get 0.1182(12).

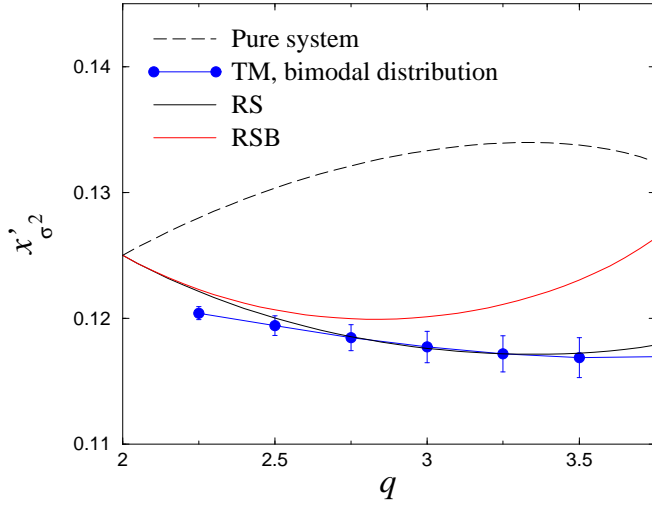


FIG. 7. Exponent of the second moment of the spin-spin correlation function as a function of the number of states of the disordered Potts model (binary disorder). The comparison is done with Replica Symmetry and Replica Symmetry Breaking scenarios [49]. The agreement with the RS result is quite good around $q = 3$. When q is close to 2, the discrepancy can be attributed to the weak relevance of disorder. We indeed used a simple exponential fit as can be expected at a stable disordered FP, but at $q = 2$, one knows from Ludwig's results that logarithmic corrections must be added. These corrections can also influence the vicinity of $q = 2$ in a numerical approach.

TABLE VI. Decay exponent of the second moment of the spin-spin correlation function compared to Replica Symmetry and Replica Symmetry Breaking expressions of Eqs. (11) and (12). The results written in bold face correspond to the range of values of q where the agreement is particularly satisfactory.

q	Perturbative results		TM result Binary Disorder
	x'_{σ^2}	x''_{σ^2}	
2.25	0.12213	0.12229	0.1204(5)
2.5	0.12002	0.12067	0.1194(8)
2.75	0.11854	0.11997	0.1185(10)
3.	0.11761	0.12011	0.1177(12)
3.25	0.11718	0.12110	0.1172(14)
3.5	0.11723	0.12304	0.1169(16)
Ternary Disorder			
3.	0.11761	0.12011	0.1182(12)
Continuous Disorder			
3.	0.11761	0.12011	0.1173(14)

C. Multifractality

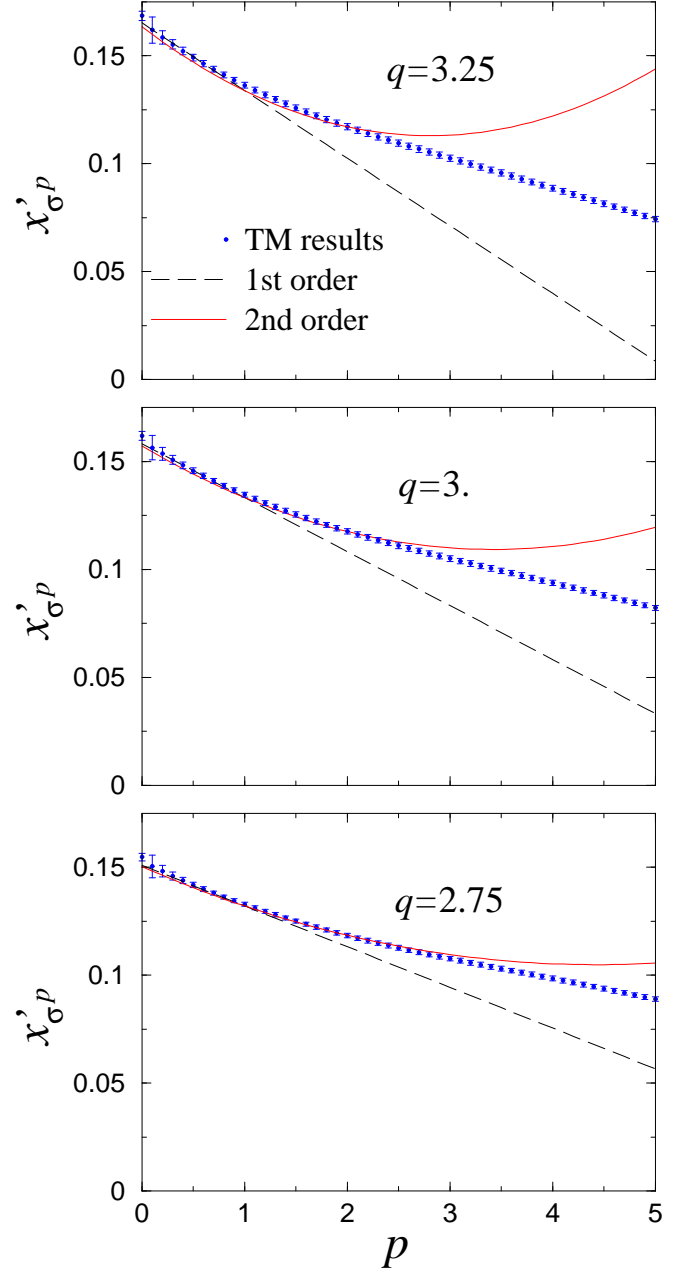


FIG. 8. Comparison of the multifractal exponents (reduced moment of the correlation function $\overline{\langle \sigma(0)\sigma(u) \rangle^p}^{1/p}$) with the second order expansion of Lewis in the RS scheme [47] for different values of q indicated in the figure (bimodal probability distribution).

The multiscaling behaviour of the spin-spin correlation functions is noticeable in the p -dependent set of exponents of the reduced moments $\overline{\langle \sigma(0)\sigma(\rho) \rangle^p}^{1/p}$. The second moment has already been computed when looking for Replica Symmetry, and it can be generalized in the

strip geometry using Eq. (21). We performed an exhaustive computation of 50 different moments in the range $0 \leq p \leq 5$ in the strip geometry, and the associated scaling dimensions followed from a semi-log fit $\ln \langle \sigma(0)\sigma(u) \rangle^p$ vs $\ln u$, according to Eq. (21), followed by an extrapolation to $L \rightarrow \infty$. Examples for $q = 2.75, 3$ and 3.25 are shown in Fig. 8 (bimodal probability distribution) where the numerical results are also compared to the first order expansion of Ludwig and to the second order expansion in the RS scheme in Eq. (10). The second order result is clearly very good up to values of p close to 3 and then breaks down as already noticed by Lewis [48].

An alternate presentation of the results (used e.g. by Ludwig [9]) is given by the scaling dimension of the moment of the correlation function itself, $\overline{\langle \sigma(0)\sigma(\rho) \rangle^p}$ (not the reduced function $\overline{\langle \sigma(0)\sigma(\rho) \rangle^{1/p}}$). The scaling dimension is thus simply $px'_{\sigma^p}(q)$, hereafter denoted by $X'_{\sigma^p}(q)$ by a simple extension of Ludwig's notation. An example, with $q = 3$, is shown in Fig. 9 where we have also shown the results obtained with the continuous probability distribution at the optimal disorder amplitude. Once again, we find a promising agreement between the numerical data and the perturbative result which confirms universality.

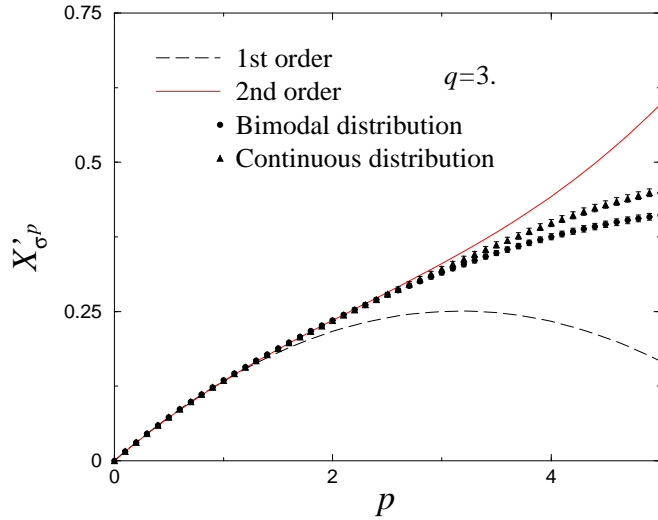


FIG. 9. Comparison of the multifractal exponents (moment of the correlation function $\overline{\langle \sigma(0)\sigma(u) \rangle^p}$) with the second order expansion of Lewis in the RS scheme [47] for both the bimodal and the continuous probability distributions.

What is interesting in this latter presentation is the link with other fields where multifractality is observed. One then usually introduces a universal function, the multiscaling function $H(\alpha)$, which is simply the Legendre transform of the set of independent scaling indexes $X'_{\sigma^p}(q)$. Setting $dX'_{\sigma^p}(q) = \alpha dp$, this function is simply obtained by $H(\alpha) = X'_{\sigma^p}(q) - \alpha p$. The geometrical interpretation of this Legendre transform follows from the relation $\frac{\partial H}{\partial \alpha} = -p$ where α is defined by $\frac{\partial X'_{\sigma^p}(q)}{\partial p} = \alpha$.

The scaling dimension $x'_{\sigma^p}(q)$ is obtained on the plot of $H(\alpha)$ by the intercept of the tangent of slope $-p$ with the abscissa axis. An example of multiscaling function $H(\alpha)$ deduced from the numerical data with the bimodal probability distribution is shown in Fig. 10 for $q = 3$ and the line of slope -2 , leading to the exponent of the second moment (See table VI) is also shown. For comparison, the function $H_{(k)}(\alpha)$ deduced from the k -th order (in y_H) perturbative results of Ludwig ($k = 1$) and Lewis ($k = 2$) (10) are also plotted. Other values of q are shown in Fig. 11.

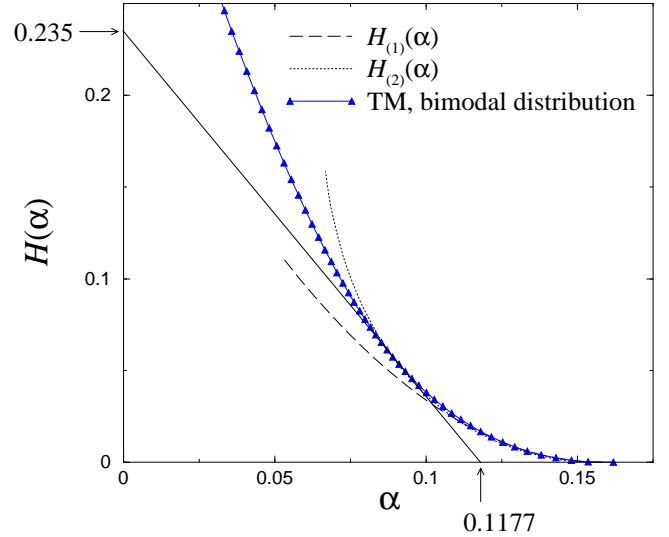


FIG. 10. Universal function $H(\alpha)$ for different $q = 3$. The functions $H_{(1)}(\alpha)$ and $H_{(2)}(\alpha)$ deduced from Eq. (10) at first or second order, respectively, are shown for comparison.

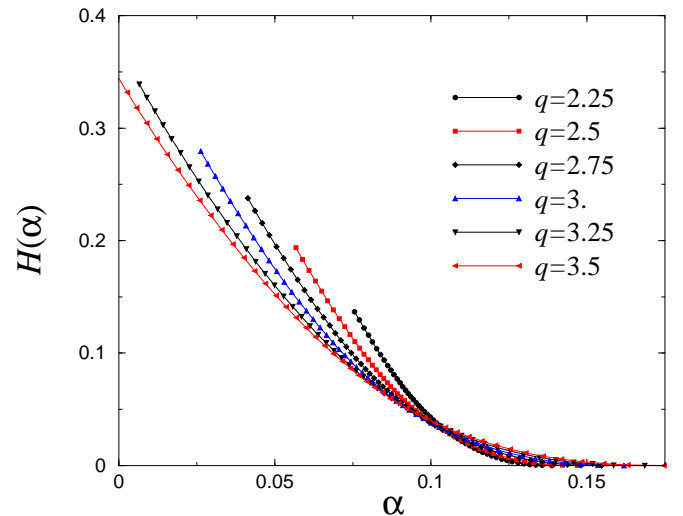


FIG. 11. Universal function $H(\alpha)$ for different values of q (bimodal probability distribution).

D. Correlation function probability distribution

In Ref. [9], Ludwig presented a remarkable discussion of the spin-spin correlation function probability distribution. He showed how all the relevant information on the large distance behaviour is encoded in the multifractal function $H(\alpha)$. In this section, we follow Ludwig's arguments and report a numerical study of the correlation function probability distribution in the cylinder geometry.

According to the results of the previous section, the moments of the spin-spin correlation function along the strip asymptotically behaves as follows:

$$\overline{G^p(u)} \equiv \overline{(\sigma(0)\sigma(u))^p} \sim B_p e^{-\frac{2\pi u}{L} X'_{\sigma^p}} \quad (34)$$

and are defined in terms of the probability distribution $\mathcal{P}[G(u)]$:

$$\overline{G^p(u)} = \int_0^1 dG(u) \mathcal{P}[G(u)] G^p(u). \quad (35)$$

Following Ludwig, we introduce the variable $Y(u) = -\ln G(u)$ and write $G^p(u) = e^{-pY(u)}$. Using the identity $\mathcal{P}[G(u)]dG = \mathcal{P}[Y(u)]dY$ and equations (34) and (35), one obtains

$$\int_0^\infty dY(u) \mathcal{P}[Y(u)] e^{-pY(u)} \sim B_p e^{-\frac{2\pi u}{L} X'_{\sigma^p}} \quad (36)$$

which leads to the expression of the probability distribution by inverting the Laplace transform ($\delta > 0$):

$$\mathcal{P}[Y(u)] = \frac{1}{2i\pi} \int_{\delta-i\infty}^{\delta+i\infty} dp B_p e^{-\frac{2\pi u}{L} [X'_{\sigma^p} - \frac{Y(u)}{2\pi u/L} p]}. \quad (37)$$

The amplitude B_p is weakly depending on p . Following Ludwig, it can be rewritten as $B_p = \exp\left[-\frac{2\pi u}{L} \left(-\frac{\ln B_p}{2\pi u/L}\right)\right]$, but can be forgotten, since it only introduces a small correction when $2\pi u/L \rightarrow \infty$. Let us define the function $h(p) = X'_{\sigma^p} - \frac{Y(u)}{2\pi u/L} p$. In the large distance limit $2\pi u/L \rightarrow \infty$, the integral can be evaluated by the saddle-point approximation at the minimum p_0 of $h(p)$:

$$\left(\frac{\partial}{\partial p} X'_{\sigma^p}\right)_{p_0} = \frac{Y(u)}{2\pi u/L} \quad (38)$$

Instead of $Y(u)$, we define the scaled variable $\alpha = \frac{Y(u)}{2\pi u/L}$, and the saddle point value at p_0 only depends on this variable $h(p_0) = H(\alpha)$, where $H(\alpha)$ is nothing but the

multifractal function defined in the previous section. We thus obtain the probability distribution

$$\mathcal{P}[Y(u)] \sim \exp\left[-\frac{2\pi u}{L} H\left(\frac{Y(u)}{2\pi u/L}\right)\right], \quad (39)$$

or, using $\mathcal{P}[Y(u)]dY = \mathcal{P}(\alpha)d\alpha$,

$$\mathcal{P}(\alpha) \sim \frac{2\pi u}{L} \exp\left[-\frac{2\pi u}{L} H(\alpha)\right]. \quad (40)$$

The multifractal function contains the essential information on the probability distribution. In order to check this expression, the value of $H(\alpha)$ at fixed α is extracted by fitting the probability distribution to the expression

$$\ln \mathcal{P}(\alpha) = \text{const} + \ln \frac{2\pi u}{L} - \frac{2\pi u}{L} H(\alpha). \quad (41)$$

It is shown in Fig. 12 where the probability distribution of the spin-spin correlation function was obtained after collecting the results over 96 000 disorder realizations in 50 classes. The values of $H(\alpha)$ are slightly too large, compared to the results presented in the previous section. We can indeed observe in Fig. 12 a deviation from the linear behaviour which would be expected with these variables, and the shorter the distance u , the larger the deviation.

This could be due to a correction to the leading behaviour given by the saddle-point approximation⁴. If we expand the function $h(p)$ close to p_0 , $h(p) \simeq H(\alpha) + \frac{1}{2}h''(p_0)(p-p_0)^2$, with $h''(p_0) > 0$ we obtain, instead of Eq. (39), the following result for the probability distribution $\mathcal{P}[Y(u)]$ [62]:

$$\mathcal{P}[Y(u)] \sim \left(\frac{2\pi u}{L}\right)^{-1/2} \exp\left[-\frac{2\pi u}{L} H\left(\frac{Y(u)}{2\pi u/L}\right)\right] \quad (42)$$

and a correction appears in $\mathcal{P}(\alpha)$:

$$\ln \mathcal{P}(\alpha) - \frac{1}{2} \ln \frac{2\pi u}{L} = \text{const} - \frac{2\pi u}{L} H(\alpha). \quad (43)$$

This is shown in Fig. 13 where a linear behaviour is now obtained in the whole range of values of u/L . A linear fit in the coordinates of Fig. 13 gives the value of the multifractal function $H(\alpha)$ which can be compared to the results of Fig. 10 obtained in section IV C. This fit is performed for all values of $0.034 < \alpha < 0.15$ for $q = 3$ for the cases of the bimodal probability distribution and of the continuous distribution. The results are shown in Fig. 14.

⁴We mention here that a possible correction to the saddle-point approximation has been suggested by Olson and Young in their study of higher values of q .

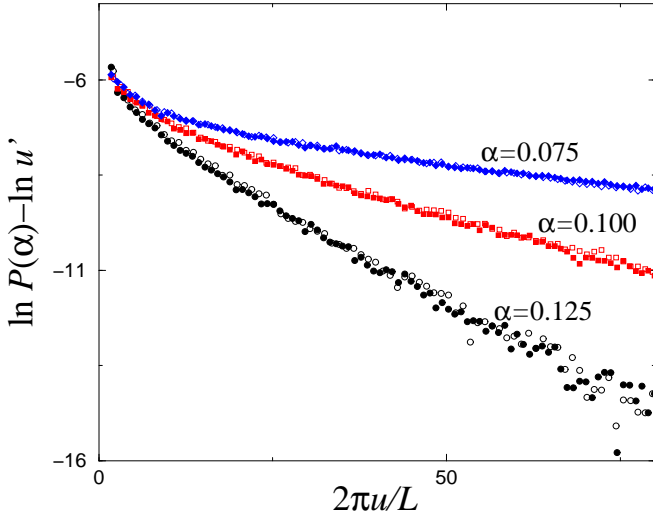


FIG. 12. Behaviour of the probability distribution $\mathcal{P}(\alpha)$ as a function of the distance along the strip $2\pi u/L$. The rescaled position along the strip is written $u' = 2\pi u/L$. Three fixed values of α are shown, the opened and filled symbols respectively correspond to the strip widths $L = 6$ and 7 . A good collapse of the data at both sizes is observed, but the behaviour displays a deviation from linearity at small distances ($q = 3$, binary distribution).

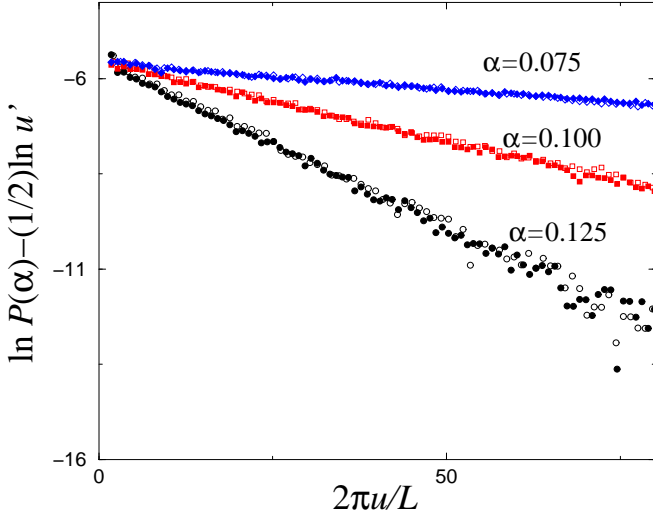


FIG. 13. Same as Fig. 12 accounting for the correction in Eq. (43) close to the saddle-point approximation.

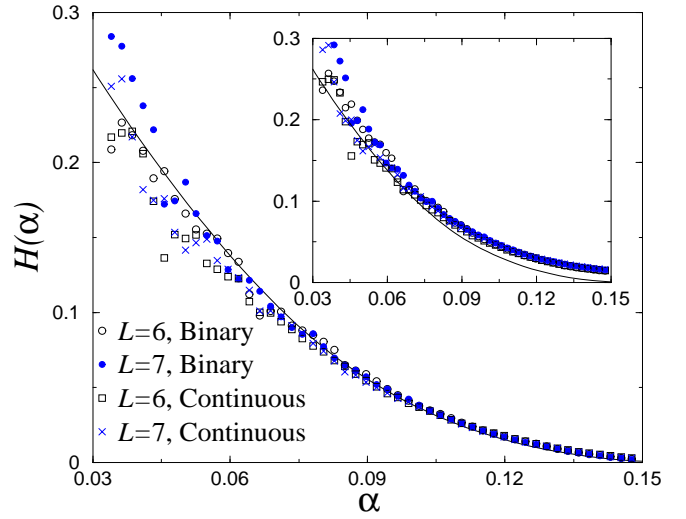


FIG. 14. Multifractal function $H(\alpha)$ as it is deduced from the fit of the probability distribution $\mathcal{P}(\alpha)$ to Eq. (43) accounting for the correction near the saddle-point approximation. It is compared to the results of Fig. 10 in solid line. The insert shows slightly too large values of $H(\alpha)$ when deduced from Eq. (41).

This latter figure shows that the correlation function probability distribution is entirely determined by the universal multifractal function $H(\alpha)$.

V. CONCLUSIONS

In this paper, we have investigated the critical behaviour of the moments of the spin-spin correlation functions of two-dimensional random bond Potts ferromagnets using Transfer Matrix techniques and conformal methods. New features of our present work are the following.

- i) As far as we know, universality of the critical behaviour of the moments of the correlation function was checked for the first time in such systems⁵. This statement follows from the numerical evidence that the scaling dimension of the average spin-spin correlation function, as well as those of higher moments or typical behaviour do not depend on the details of the probability distribution, provided that the computations are performed at the disordered fixed point given by the maximum condition of the central charge. The exponent of the average correlation function is furthermore in

⁵We mention here that a MC study in the first-order regime of the pure model ($q = 5$) was recently reported where random bond disorder and dilution were found to belong to the same universality class [63].

very good agreement with theoretical results using perturbative conformal field theory available in the literature.

- ii) The question of a possible breaking of Replica Symmetry is also considered and the numerical data strongly support the absence of Replica Symmetry Breaking. The problem is investigated through the comparison of the scaling dimension of the second moment of the correlation function, which is compared to perturbative results obtained within both schemes. Although previous numerical results (using Monte Carlo simulations) which led to similar conclusions were already reported at $q = 3$, we believe that our study is conclusive, since it extends the work to other non integer values of q .
- iii) The multiscaling behaviour of the spin-spin correlation function is investigated. The exponential decay of the moments of the correlation functions along very long strips is used to deduce numerically the corresponding critical exponents. These dimensions continuously depend on the moment order, as a consequence of multifractality. They are furthermore very weakly dependent of the probability distribution. At low moment order, the numerical results are furthermore in agreement with a perturbative result obtained within the Replica Symmetry scheme. When the moment order increases, a discrepancy is observed, resulting from the lack of validity of the perturbation expansion, and possibly of a numerical determination which becomes less precise. The multifractal function, given by the Legendre transform of the set of independent scaling dimensions is also computed for different values of q . It is shown that this universal function completely determines the shape of the correlation function probability distribution.

The main result of this paper is probably to show that universality in random systems has to be understood in the sense of a critical behaviour which does not depend on the choice of the probability distribution (this is only true up to some extent, since special distributions which do not obey the central limit theorem, like Levy flights, would certainly lead to different results). By critical behaviour, here we mean the behaviour of all the moments of a physical quantity, entirely contained in the multifractal function or the correlation function probability distribution but we want to stress that lack of self-averaging does not imply absence of universality.

We also note that logarithmic corrections were recently reported in the disconnected energy-energy correlations function [64] and that disorder was shown to induce non-vanishing cross-correlations between spin-spin and energy-energy moments [65]. The multiscaling of energy correlations has been studied very recently by J.L. Jacobsen [66].

ACKNOWLEDGMENTS

We would like to thank M.A. Lewis and I. Campbell for stimulating discussions. The computations were performed on the *SP2* at the CNUSC in Montpellier under project No. C990011, and the *Power Challenge Array* at the CCH in Nancy.

-
- [1] V.S. Dotsenko, *Physics-Uspekhi* **38**, 457 (1995).
 - [2] A. Aharony and A.B. Harris, *Phys. Rev. Lett.* **77**, 3700 (1996).
 - [3] B. Derrida, *Phys. Rep.* **103**, 29 (1984).
 - [4] S. Wiseman and E. Domany, *Phys. Rev. Lett.* **81**, 22 (1998).
 - [5] S. Wiseman and E. Domany, *Phys. Rev. E* **58**, 2938 (1998).
 - [6] H.E. Stanley and P. Meakin, *Nature* **335**, 405 (1988).
 - [7] M. Janssen, *Int. J. Mod. Phys. B* **8**, 943 (1994).
 - [8] A.W.W. Ludwig, *Nucl. Phys. B* **285** [FS19], 97 (1987).
 - [9] A.W.W. Ludwig, *Nucl. Phys. B* **330**, 639 (1990).
 - [10] A.W.W. Ludwig and J.L. Cardy, *Nucl. Phys. B* **330** [FS19], 687 (1987).
 - [11] S. Wiseman and E. Domany, *Phys. Rev. E* **51**, 3074 (1995).
 - [12] M. Picco, *Phys. Rev. B* **54**, 14 930 (1996).
 - [13] J.K. Kim, *Phys. Rev. B* **53**, 3388 (1996).
 - [14] M. Picco, e-print cond-mat/9802092.
 - [15] J.L. Jacobsen and J.L. Cardy, *Nucl. Phys. B* **515**, 701 (1998).
 - [16] U. Glaus, *J. Phys. A* **20**, L595 (1987).
 - [17] M. Picco, *Phys. Rev. Lett.* **79**, 2998 (1997).
 - [18] J.L. Cardy and J.L. Jacobsen, *Phys. Rev. Lett.* **79**, 4063 (1997).
 - [19] C. Chatelain and B. Berche, *Phys. Rev. E* **60**, 3853 (1999).
 - [20] G. Palágyi, C. Chatelain, B. Berche and F. Igloi, e-print cond-mat/9906067.
 - [21] T. Olson and A.P. Young, *Phys. Rev. B* **60**, 3428 (1999).
 - [22] C. Chatelain and B. Berche, *Phys. Rev. E* **58**, R6899 (1998).
 - [23] P.W. Kasteleyn and C.M. Fortuin, *J. Phys. Soc. Japan* **26** Suppl., 11 (1969).
 - [24] H.W.J. Blöte and M.P. Nightingale, *Physica (Amsterdam)* **112A**, 405 (1982).
 - [25] A.B. Harris, *J. Phys. C* **7**, 1671 (1974).
 - [26] V.S. Dotsenko and V.I.S. Dotsenko, *Adv. Phys.* **32**, 129 (1983).
 - [27] B.N. Shalaev, *Sov. Phys. Solid State* **26**, 1811 (1984).
 - [28] R. Shankar, *Phys. Rev. Lett.* **58**, 2466 (1987).
 - [29] R. Shankar, *Phys. Rev. Lett.* **61**, 2390 (1988).
 - [30] A.W.W. Ludwig, *Phys. Rev. Lett.* **61**, 2388 (1988).
 - [31] B.N. Shalaev, *Phys. Rep.* **237**, 129 (1994).
 - [32] J.S. Wang, W. Selke, V.I.S. Dotsenko and V.B. Andreichenko, *Europhys. Lett.* **11**, 301 (1990).

- [33] V.B. Andreichenko, V.I.S. Dotsenko, W. Selke and J.S. Wang, Nucl. Phys. B **344**, 531 (1990).
- [34] A.L. Talapov and L.N. Shchur, Europhys. Lett. **27**, 193 (1994).
- [35] A. Roder, J. Adler and W. Janke, Phys. Rev. Lett. **80**, 4697 (1998).
- [36] A. Roder, J. Adler and W. Janke, Physica A **265**, 28 (1999).
- [37] G. Mazzeo and R. Kühn, Phys. Rev. E **60**, 3823 (1999).
- [38] V.N. Plechko, Phys. Lett. A **239**, 289 (1998).
- [39] S.L.A. de Queiroz, Phys. Rev. E **51**, 1030 (1995).
- [40] S.L.A. de Queiroz and R.B. Stinchcombe, Phys. Rev. E **54**, 190 (1996).
- [41] P. Lajkó and F. Igloi, e-print cond-mat/9908376.
- [42] M.P.M. den Nijs, J. Phys. A **12**, 1857 (1979).
- [43] B. Nienhuis, J. Phys. A **15**, 199 (1982).
- [44] V.I.S. Dotsenko and V.A. Fateev, Nucl. Phys. B **240** [FS12], 312 (1984).
- [45] G. Jug and B.N. Shalaev, Phys. Rev. B **54**, 3442 (1996).
- [46] V.I. Dotsenko, M. Picco and P. Pujol, Nucl. Phys. B **455** [FS], 701 (1995).
- [47] M.A. Lewis, Europhys. Lett. **43**, 189 (1998), Erratum, Europhys. Lett. **47**, 129 (1999).
- [48] M.A. Lewis, e-print cond-mat/9905401.
- [49] V.I. Dotsenko, V.I. Dotsenko and M. Picco, Nucl. Phys. B **250**, 633 (1998).
- [50] V.I. Dotsenko, V.I. Dotsenko, M. Picco and P. Pujol, Europhys. Lett. **32**, 425 (1995).
- [51] L. Chayes and K. Shtengel, e-print cond-mat/981103
- [52] V.I. Dotsenko, J.L. Jacobsen, M.A. Lewis, and M. Picco, e-print cond-mat/9812227.
- [53] A.B. Zamolodchikov, JETP Lett. **43**, 730 (1986).
- [54] H. Furstenberg, Trans. Am. Math. Soc. **108**, 377 (1963).
- [55] N. Sourlas, e-print cond-mat/9811406.
- [56] J.L. Jacobsen and M. Picco, e-print cond-mat/9910071.
- [57] M. Mézard, G. Parisi and M.A. Virasoro, Spin Glass Theory and beyond, World Scientific (Singapore, 1987).
- [58] E. Marinari, G. Parisi, J. Ruiz-Lorenzo and F. Ritort, Phys. Rev. Lett. **76**, 843 (1996).
- [59] E. Marinari, C. Naitza, F. Zuliani, G. Parisi, M. Picco and F. Ritort, Phys. Rev. Lett. **81**, 1698 (1999).
- [60] H. Bokil, A.J. Bray, B. Drossel and M.A. Moore, Phys. Rev. Lett. **82**, 5174 (1999).
- [61] E. Marinari, C. Naitza, F. Zuliani, G. Parisi, M. Picco and F. Ritort, Phys. Rev. Lett. **82**, 5175 (1999).
- [62] N.G. De Bruijn, Asymptotic methods in analysis, Dover, New-York, 1981.
- [63] R. Paredes and J. Valbuena, Phys. Rev. E **59**, 6275 (1999).
- [64] J.L. Cardy, e-print cond-mat/9911024.
- [65] T. Davis and J.L. Cardy, e-print cond-mat/9911083.
- [66] J.L. Jacobsen, e-print cond-mat/9912304.